

Neoclassical tearing mode stabilization by electron cyclotron current drive for HL-2M tokamak

Jing-Chun Li(李景春), Jia-Qi Dong(董家齐), Xiao-Quan Ji(季小全), and You-Jun Hu(胡友俊)
Citation: Chin. Phys. B, 2021, 30 (**7**): 075203. DOI: 10.1088/1674-1056/abfb52
Journal homepage: http://cpb.iphy.ac.cn; http://iopscience.iop.org/cpb

What follows is a list of articles you may be interested in

Basic features of the multiscale interaction between tearing modes and slab ion-temperature-gradient modes

L Wei(魏来), Z X Wang(王正汹), J Q Li(李继全), Z Q Hu(胡朝清), Y Kishimoto(岸本泰明)
Chin. Phys. B, 2019, 28 (**12**): 125203. DOI: 10.1088/1674-1056/ab5437

Effects of resonant magnetic perturbation on the instability of single tearing mode with non-shear flow

Le Wang(王乐), Ming Yang(阳明), Wen-Bin Lin(林文斌)
Chin. Phys. B, 2019, 28 (**1**): 015203. DOI: 10.1088/1674-1056/28/1/015203

Numerical analysis of the optimized performance of the electron cyclotron wave system in a HL-2M tokamak

Jing-Chun Li(李景春), Xue-Yu Gong(龚学余), Jia-Qi Dong(董家齐), Jun Wang(王俊), Lan Yin(尹岚)
Chin. Phys. B, 2016, 25 (**4**): 045201. DOI: 10.1088/1674-1056/25/4/045201

Optimized calculation of the synergy conditions between electron cyclotron current drive and lower hybrid current drive on EAST

Wei Wei(韦维), Bo-Jiang Ding(丁伯江), Y Peysson, J Decker, Miao-Hui Li(李妙辉),Xin-Jun Zhang(张新军), Xiao-Jie Wang(王晓洁), Lei Zhang(张磊)
Chin. Phys. B, 2016, 25 (**1**): 015201. DOI: 10.1088/1674-1056/25/1/015201

Numerical study of fast ion behavior in the presence of magnetic islands and toroidal field ripple in the EAST tokamak

Zhang Wei, Hu Li-Qun, Sun You-Wen, Ding Si-Ye, Zhang Zi-Jun, Liu Song-Lin
Chin. Phys. B, 2014, 23 (**10**): 105201. DOI: 10.1088/1674-1056/23/10/105201

Neoclassical tearing mode stabilization by electron cyclotron current drive for HL-2M tokamak*

Jing-Chun Li(李景春)[1,2,†], Jia-Qi Dong(董家齐)[3], Xiao-Quan Ji(季小全)[3], and You-Jun Hu(胡友俊)[4]

[1] Department of Earth and Space Sciences, Southern University of Science and Technology, Shenzhen 518000, China
[2] University of California, Irvine, California 92697, USA
[3] Southwestern Institute of Physics, Chengdu 610041, China
[4] Institute of Plasma Physics, Chinese Academy of Sciences, Hefei 230031, China

(Received 12 March 2021; revised manuscript received 19 April 2021; accepted manuscript online 26 April 2021)

Investigation of neoclassical tearing mode and its suppression by electron cyclotron current drive (ECCD) has been carried out in HL-2M tokamak. The current driving capability of the electron cyclotron wave is evaluated. It is found that the deposition location can be effectively controlled by changing the poloidal angle. The validation of electron cyclotron wave heating and current driving has been demonstrated for the upper launcher port. We show that 3.0 MW and 2.5 MW modulated ECCD can completely stabilize (2,1) and (3,2) NTMs, respectively. The non-modulated ECCD, radial misalignment as well as current profile broadening have deleterious effect on the NTM stabilization. The time required for suppression of (3,2) mode is shorter than that required for the suppression of (2,1) mode. Moreover, the time needed for complete stabilization at different initial island width has been quantitatively presented and analyzed.

Keywords: neoclassical tearing mode, magnetic island, electron cyclotron current drive, numerical modelling

PACS: 52.35.Hr, 52.55.Fa, 52.55.Wq, 52.35.Py **DOI:** 10.1088/1674-1056/abfb52

1. Introduction

Tearing modes are instabilities caused by magnetic reconnection. Neoclassical tearing mode (NTM) is a new tearing instability in toroidal plasma, which appears and is recognized as a factor to degrade plasma performance and may even lead to disruptions when the driven force of bootstrap current is considered.[1–4] So far, people have come up with many ways to inhibit NTM, including the use of electron cyclotron current drive (ECCD),[5,6] lower hybrid current drive,[7,8] externally applied resonant magnetic perturbations,[9,10] neutral beam injection, as well as using plasma rotation. Among those, ECCD is one of the most effective ways since it can deposit current in plasma region flexibly, and the current drive efficiency can reach a high level as well.[11] This paper will focus on NTM stabilization by ECCD in HL-2M tokamak configuration.

Presently, many devices such as DIII-D, ASDEX Upgrade,[12,13] and JT-60U[14] have shown the suppression of neoclassical tearing modes (NTM) with ECCD. The tearing mode was successfully suppressed on the HL-2A device.[15] Investigation on $m/n = 1/1$ internal mode coupling to produce NTM is also carried out on EAST.[16] Since 2012, research on real-time control of NTM has been conducted on DIII-D. In this case, the gyrotron remains closed until NTM is detected. The gyrotron is immediately opened to suppress NTM when NTM is detected. If detection and alignment are early enough, this technique could quickly suppress NTM. Experiments have found that an increase in the fusion gain factor, Q, can be observed when NTM plus ECCD is applied.[17] In addition, recent experiments show that fueling deuterium pellets can partially stabilize the $m/n = 2/1$ NTM. Corresponding Modified Rutherford's equation (MRE) calculations show that the ECCD current required for complete NTM stabilization will be greatly reduced when transportation is enhanced at O-point.[18] Theoretically, there are three ways to study the NTM and its suppression by ECCD. One is to use the generalized Rutherford equation (GRE)[19,20] to study the evolution of the island width w, and the effect of ECCD on NTM. The second to solve the nonlinear MHD equation to describe the island behavior.[21,22] The third is to use the Vlasov gyro-kinetic code to study non-linear evolution of a magnetic island.[23] The magnetic island is a system with multiple spatial scales for the third case. In tokamak, the poloidal wavelength of the island is the order of the minor radius, and its width can be order of the ion Larmor radius or smaller. For this reason, the dynamic of tearing mode has been studied in the past using gyro-kinetic theory. Recent gyrokinetic study also has found that turbulence can provide seed magnetic islands for NTM by creating magnetic structures of ion gyroradius scale in radial direction, and NTM can bypass the linear growth phase. However, in general, for the suppression of NTM, the fluid

*Project supported by the National Key Research and Development Program of China (Grant Nos. 2018YFE0303102, 2018YFE0301100, and 2017YFE0301702), the National Natural Science Foundation of China (Grant Nos. 11905109 and 11947238), U.S. DOE SciDAC ISEP, users with Excellence Program (on EAST tokamak) of Hefei Science Center CAS under (Grant No. 2021HSC-UE017), and the Center for Computational Science and Engineering of Southern University of Science and Technology.

†Corresponding author. E-mail: lijc@sustech.edu.cn

© 2021 Chinese Physical Society and IOP Publishing Ltd

model is sufficiently accurate.[24] In addition, since the time scale is quite large when calculating the evolution of NTM using gyrokinetics, the simulation of kinetics will consume considerable computing resources. In addition, the calculation accuracy is also particularly high in order to ensure the convergence of long-term calculations. Surely, the advantage of kinetic simulation is that it can accurately study the evolution of the magnetic island in high-temperature plasma, and study the influence of kinetic effects of ions on the evolution of the magnetic island.[25]

HL-2M is a new medium-sized tokamak being manufactured by SWIP. It is committed to supporting the key physics and technology research of ITER and CFETR[26]. The first discharge was carried out at the end of 2020. HL-2M is designed to have high β value, and it takes advantage of the separable toroidal field (TF) coil to improve the plasma performance, thus exploring the technical and engineering potential of ITER and future fusion reactors.[27,28] Since HL-2M is expected to have high fraction of bootstrap current, the NTM on it will be extremely destructive. Currently, the NTM real-time control system on HL-2M is also under construction. It is necessary to simulate the evolution and suppression of NTM before the experiment to provide a certain reference to the upcoming experiments.

In this paper, we will study the NTM and its stabilization with coupling ray-tracing code and MHD code. It is found that the deposition location can be effectively controlled by changing the poloidal angle. We show that 3.0 MW and 2.5 MW modulated ECCD can completely stabilize (2,1) and (3,2) NTMs, respectively. The non-modulated ECCD, radial misalignment as well as current profile broadening have deleterious effect on the NTM stabilization. The time required for suppression of (3,2) mode is shorter than that required for the suppression of (2,1) mode. In addition, the time needed for complete stabilization at different initial island width has also been quantitatively presented.

The rest of this paper is organized as follows. The model of ray-tracing code and NTM fluid equation is introduced in Section 2. In Section 3, we report the results of numerical study for electron cyclotron wave heating and current drive, and the process of NTM stabilization in HL-2M configuration. Brief conclusions are given in Section 4.

2. Modeling

2.1. TORAY code

We use the TORAY code to calculate the trajectories of the electron cyclotron wave and the driven current. TORAY uses the dispersion relation of cold plasma to simulate wave trajectories. Two models (Cohen and Lin-Liu *et al.*[29]) could be used to calculate ECCD in general geometry. TORAY code mainly solves the wave ray-tracing equation

$$\frac{\mathrm{d}\boldsymbol{x}}{\mathrm{d}s} = -\frac{\partial D/\partial k}{|\partial D/\partial k|}; \tag{1}$$

$$\frac{\mathrm{d}k}{\mathrm{d}s} = \frac{\partial D/\partial \boldsymbol{x}}{|\partial D/\partial k|}; \tag{2}$$

where s is the arc length along the ray path, k is the wave number, $\boldsymbol{x}$ is the spatial position, and D is the real part determined from the dispersion relation given by a cold plasma approximation, $D(k, w_r, x) = 0$, where w_r is the wave frequency. The ECW power absorbed by the plasma is given by the integral along the ray path

$$p(s) = 1 - \exp\left(-2\int_0^s \mathrm{Im}(k)\cdot\frac{\mathrm{d}\boldsymbol{x}}{\mathrm{d}s}\right), \tag{3}$$

where the imaginary part of k is obtained from solving the dispersion relation. For ECCD, Cohen model includes relativistic, electron–ion collisions, and trapped particle effects. Lin-Liu has noted that the current drive efficiency, J/P_d, which calculates the ECCD, requires division by $\langle B\rangle$. This is approximately accurate by dividing J/P_d with $1+\varepsilon$, where ε is the inverse aspect ratio $(B_\mathrm{max}B_\mathrm{min})/(B_\mathrm{max}+B_\mathrm{min})$ of device, since $\langle B\rangle$ is not currently available to TORAY.

At present, TORAY has been performed a series of benchmarks against other linear and quasi-linear ray-tracing codes, such as Gaussian beam codes, and quasi-optical codes.[30–32] Here in this work, we use thirty rays with different Gaussian distributions, and adopt the Lin-Liu model to calculate the current drive efficiency. The beam width is 2 cm. For TORAY, the poloidal injection angle α refers to the angle measured from the vertical direction counter-clock-wisely. The toroidal injection angle β refers to the angle measured counterclockwise along the major radius on the equatorial plane at the launching point.

2.2. Model for neoclassical tearing mode

The growth rate of NTM is calculated by the TM8 code in this paper, namely, we solve following MHD equations in a cylindrical configuration:[33]

$$\frac{\mathrm{d}\psi}{\mathrm{d}t} = E - \eta(j - j_\mathrm{b} - j_\mathrm{d}), \tag{4}$$

$$\rho\left(\frac{\partial}{\partial t} + \boldsymbol{\nu}\cdot\nabla\right)\nabla^2\phi = \boldsymbol{e}_\mathrm{t}\cdot(\nabla\psi\times\nabla j) + \mu_\perp\rho\nabla^4\phi, \tag{5}$$

$$\frac{3}{2}\frac{\mathrm{d}p}{\mathrm{d}t} = \nabla\cdot(\chi_\parallel\nabla_\parallel p) + \nabla\cdot(\chi_\perp\nabla_\perp p) + Q, \tag{6}$$

where $(\mathrm{d}/\mathrm{d}t) = (\partial/\partial t) + \boldsymbol{\nu}\cdot\nabla$, $\boldsymbol{\nu} = \nabla\phi\times\boldsymbol{e}_\mathrm{t}$, $j = \nabla^2\psi - 2nB_{0\mathrm{t}}/(mR)$ being the toroidal plasma current density, $j_\mathrm{b} = -c_\mathrm{b}(\varepsilon^{1/2}/B_\mathrm{p})n_\mathrm{e}\,\mathrm{d}T_\mathrm{e}/\mathrm{d}r$ being the bootstrap current density calculated from electron temperature T_e self-consistently, where c_b in the expression of j_b is a constant of the order of unity, and j_d is the radio frequency (RF) driven current density along the $\boldsymbol{e}_\mathrm{t}$ direction. E is the equilibrium electric field; μ is

the plasma viscosity; $B_{\rm p}$ is the poloidal magnetic field; ρ is the plasma mass density; p is the plasma pressure; $\varepsilon = r/R$ is the inverse aspect ratio. $\chi_\perp$ and $\chi_\parallel$ are the perpendicular and parallel transport coefficients, and Q is the heating power. For TM8, the normalization scheme is as follows: the length to the minor radius a, the time t to τ_R, the helical flux to $aB_{0\rm t}$, v to a/τ_R, and $T_{\rm e}$ and $n_{\rm e}$ to their values at the magnetic axis, where $\tau_R = a^2\mu_0/\eta$ is the resistive time.

Meanwhile, we consider the transport of fast electron

$$\frac{\partial n_{\rm f}}{\partial t} = \nabla\cdot(\chi_{\parallel{\rm f}}\nabla_\parallel n_{\rm f}) + \nabla\cdot(\chi_{\perp{\rm f}}\nabla_\perp n_{\rm f}) + v_{\rm f}(n_{\rm fs} - n_{\rm f}), \quad (7)$$

where $\chi_{\perp{\rm f}}$ and $\chi_{\parallel{\rm f}}$ are the perpendicular and parallel transport coefficients of the fast electrons, and $1/v_{\rm f}$ is the slow down time of the fast electrons. The effect of electron cyclotron current drive on NTM is entered through the fast electron source term, and the fast electron source density $n_{\rm fs}$ due to the EC waves is expressed as

$$n_{\rm fs} = n_{\rm fs0}\exp\left(-\frac{(r-r_{\rm cd})^2}{w_{\rm cd}^2}\right)\Pi(h_0,\Delta h_{\rm EC}), \quad (8)$$

where $r_{\rm cd}$ is the central RF deposition point; $w_{\rm cd}$ denotes the RF characteristic width; $\Pi(h_0,\Delta h_{\rm EC})$ is a square box function for considering the wave deposition profile along the helical angle $h = m\theta + n\xi$. We set $\Pi(h_0,\Delta h_{\rm EC}) = 1$ for $h_{\rm on} < h_0 < h_{\rm off}$, and $\Pi(h_0,\Delta h_{\rm EC}) = 0$ elsewhere. h_0 is the ECW deposition center and is computed in each time step to compare with that of the magnetic island. $\Delta h_{\rm EC} = m\delta\theta + n\delta\xi$, is the instantaneous wave deposition width along the helical angle h. Besides, we set $h_{\rm on} = -\pi$ and $h_{\rm off} = \pi$ for non-modulated current drive (NMCD), and $h_{\rm on} = -\pi/2$ and $h_{\rm off} = \pi/2$ for modulated current drive (MCD) which means h_0 only varies in the half period from $-\pi/2$ to $\pi/2$ in MCD cases.

3. Numerical results

Now we use the two modeling to investigate the evolution of NTM and the effect of ECCD on it. The two models couples through Eqs. (4) and (7).

3.1. ECW power absorption and current drive in HL-2M

Firstly, we use TORAY to evaluate the ECW heating and current drive performance under HL-2M configuration. The HL-2M tokamak parameters are as follows: plasma major radius $R = 1.78$ m, minor radius $a = 0.65$ m, the toroidal magnetic field $B_{\rm t} = 2.2$ T, plasma current $I_{\rm P} = 1.2$ MA, elongation $\kappa = 1.87$, and triangularity $\delta = 0.45$. The scenarios of the single-null diverted HL-2M equilibria are constructed with the EFIT code.[34] The plasma density and temperature profiles are given as

$$n_{\rm e} = (n_{\rm ec} - n_{\rm ea})\left[1-(r/a)^i\right]^s + n_{\rm ea},$$

$$T_{\rm e} = (T_{\rm ec} - T_{\rm ea})\left[1-(r/a)^i\right]^s + T_{\rm ea}, \quad (9)$$

where $n_{\rm ec}$ ($T_{\rm ec}$) and $n_{\rm ea}$ ($T_{\rm ea}$) are the electron density (temperature) in core and at edge, respectively. $i = 1$ and $s = 1/3$ are the empirical indexes. We set $n_{\rm ec} = 6.0\times10^{19}$ m^{-3}, $n_{\rm ea} = 1.5\times10^{19}$ m^{-3}, $T_{\rm ec} = 6$ keV, $T_{\rm ea} = 0.05$ keV. The effective charge $Z_{\rm eff} = 1.8$ with a flat profile is assumed.

Shown in Fig. 1 is the HL-2M equilibrium, as well as the electron cyclotron wave trajectories on a poloidal plane. The pink lines in Figs. 1(a) and 1(b) are the contours of the helical flux surfaces of (2,1) and (3,2) magnetic islands. The electron cyclotron wave is injected from the upper launcher port. For the 2/1 mode, the rational surface location is at $\rho = 0.58$, where $\rho = (\phi/\phi_{\rm max})^{1/2}$ is the square root of normalized toroidal flux, and the required poloidal injection angle is about 120°. For the 3/2 mode, the inner side is closer to the plasma center, and the poloidal injection angle needs to be increased (the corresponding poloidal injection angle in the Fig. 1(b) is 128°), the wave can be deposited near the rational surface of $\rho = 0.46$. Therefore, for NTM suppression, the issue of radial misalignment could basically be solved by adjusting the poloidal injection angle in experiments. From the results of the previous injection angle scanning, to cover the radial range of $\rho = 0.5$–0.9, the required poloidal injection angle range is about 30° (from 98° to 128°).[35]

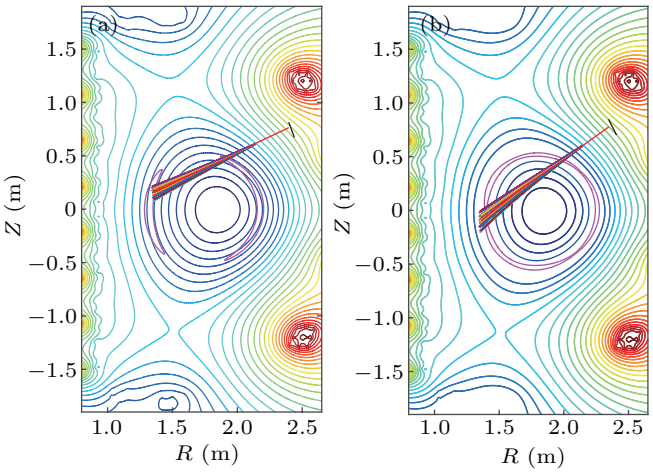


Fig. 1. The HL-2M equilibrium, and the electron cyclotron wave trajectories on a poloidal plane. The pink line in (a) and (b) are the contours of the helical flux surfaces of (2,1) and (3,2) magnetic islands.

Figure 2 shows a radial profiles of ECW power deposition and driven current density with different poloidal injection angles of 120° and 128°. The power absorption and driven current in Fig. 2 corresponds to the wave trajectories in Fig. 1. It can be seen that the increment of the poloidal angle also increases the current drive efficiency to some extent. In both cases, the absorption of wave power is 100%. The ECCD efficiency ($n(20)R(\rm m)I(\rm A)/P(\rm W)$) in the two cases with poloidal angles of 120° and 128° is about 0.011 and 0.014×10^{20} A/W/m^2, respectively. Since our focus here is

on the suppression of NTM by ECCD, we will not give more calculation results of ECCD in the HL-2M configuration. One can refer to Ref. [35] for more detailed calculations. However, we could still make a summary: (i) Increasing the poloidal angle moves the wave deposition position to the plasma core; (ii) Both adjusting the toroidal angle (within a certain range) and increasing the plasma core temperature increase the current drive efficiency of the wave; (iii) Wave injected from the upper launcher port drives larger plasma current than mid-plane injection. Therefore, an upper launcher port has been designed for the ECW system in HL-2M.

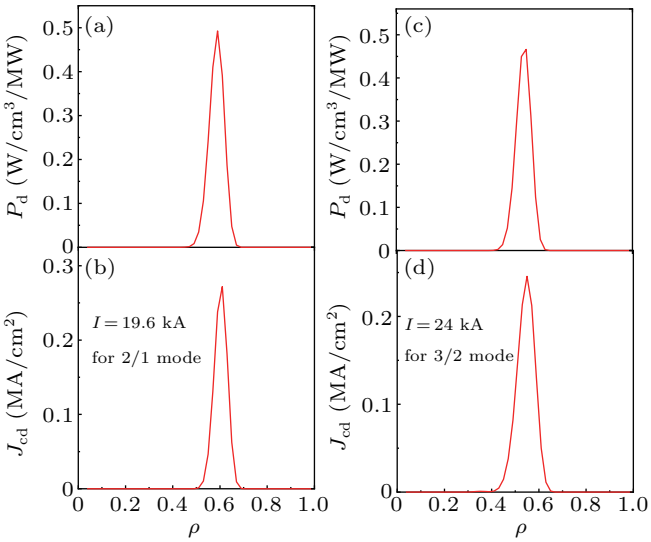


Fig. 2. Radial profile of ECW power deposition and driven current density with different poloidal injection angles 120° (a), (b) and 128° (c), (d).

3.2. Neoclassical tearing mode stabilization

Now we substitute the driven current calculated in the previous section into Eqs. (6) and (7) to simulate the process of NTM suppression. Table 1 shows the input parameters of the TM8 codes. It should be noted that the poloidal angles have been adjusted in order to guarantee that the current density is deposited on the rational surface, and the w_{cd} in Table 1 is the half-width of current density profile.

Table 1. Simulation parameters.

modes	2/1 mode	3/2 mode
r_s (a)	0.58	0.46
T_e (KeV)	2.4	3.4
n_e (m^{-3})	3.06×10^{19}	3.23×10^{19}
S	7.8×10^{7}	1.3×10^{8}
τ_R (s)	26.3	30.5
f_{BS}	0.31	0.19
$\chi_\perp$ (a^2/τ_R)	25.8	35.3
$\chi_\parallel$ (a^2/τ_R)	6.9×10^{9}	3.8×10^{9}
η_{cd} (kA/MW)	19.6	26
w_{cd} (a)	0.078	0.086

In order to study the stabilization of NTM, we first explore the influence of ECCD on NTM by changing the amplitudes of driven current. Figure 3 presents the evolution of the NTM magnetic island in different cases. The black line corresponds to the modulated ECCD cases with input wave power $P = 3$ MW, the red dotted line to the non-modulated ECCD case with input wave power $P = 3.0$ MW. In the modulated case, it indicates that 3MW ECW fully stabilizes the (2,1) NTM mode. Increasing the ECW power reduces the time needed for the complete suppress of NTM, while reducing the ECW power leads to the incomplete stabilization of NTM, and makes the magnetic island width saturated at a moderate value. On the other hand, the ECW power (3 MW) that is enough to control (2,1) NTM in modulated case cannot fully stabilize the NTM in the non-modulated case. Higher ECW power is needed for NTM suppression with NMCD. It is also worth pointing out that the saturation magnetic island width of the NTM in the simulation is $0.34a$ when there is no ECCD. Compared with the magnetic island width in HL-2A ($\sim 0.14a$), this value is larger, but it is reasonable because HL-2M is set to be high β plasma, and has a larger fraction of bootstrap current, and, therefore, the saturation width of magnetic island is relatively large.

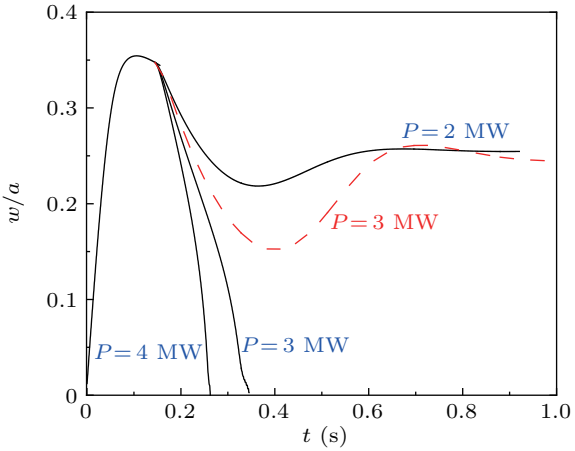


Fig. 3. The evolution of the NTM magnetic island width in different cases: the black lines correspond to the modulated ECCD cases with different wave input power, the red dotted line to the non-modulated ECCD case with wave input power $P = 3.0$ MW.

Figure 4 depicts the evolution of the (2,1) NTM magnetic island of lager characteristic width w_{cd} and during radial misalignment ECCD. It can be seen that when the radial deviation reaches a quarter of half-width of the current profile, the ECW power, that can completely stabilize the NTM in absence of deviation, no longer fully suppress the (2,1) NTM, but only reduces the saturation width of the magnetic island to a lower level. The value of this lower level is $0.05a$ in our calculations. In addition, increasing the half-width of the current profile also reduces the effect of NTM suppression. The 3 MW ECCD decreases the island width to $0.25a$ only when w_{cd} is increased by 0.5 times. The NTM suppression effect is sensitive to the width of driven current profile. Our previous simulation with scanning of the poloidal injection angle indicates that a smaller

poloidal injection angle corresponds to a larger ECCD characteristic width when the ECW wave is launched in the upper launch port. Therefore, ECW emission with a large poloidal injection angle is beneficial to NTM suppression.

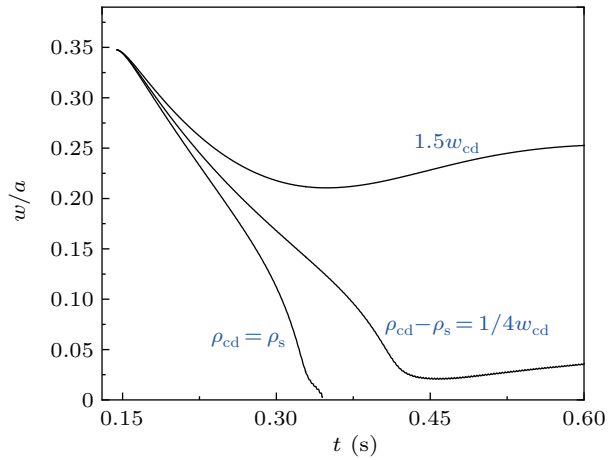


Fig. 4. The evolution of the (2,1) NTM magnetic island width with radial misalignment ECCD and lager characteristic width, w_{cd}.

Figure 5 shows the evolution of the (3,2) NTM magnetic island in different ECW power level with both modulated and non-modulated ECCD. It is shown that after linear growth of (3, 2) NTM mode, the magnetic island width at saturation is $0.115a$ without ECCD. 2.5 MW ECCD completely suppresses NTM, and 1 MW ECW power only reduces the island width to its 1/4 in the MCD cases; 3 MW ECW power quickly reduces the island width to zero. 2.5 MW of non-modulated current does not completely stabilize NTM, and only reduces the size of the magnetic island to its 3/4. More EC wave power input is needed in this case in order to fully suppress the magnetic island.

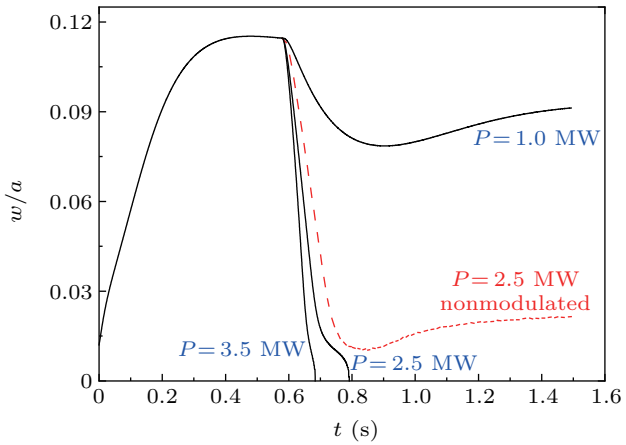


Fig. 5. The same as in Fig. 3, but for (3,2) NTM stabilization.

Figure 6 gives the same plot as in Fig. 4, but for (3,2) NTM, for which the influence of radial mismatch and current profile width on NTM suppression effect is similar to that of (2,1) mode. Increasing of the current profile width and radial deviation increase power threshold for complete suppression of NTM. However, the current profile width and radial deviation has weaker influence on the (3,2) mode suppression than they do on (2,1) mode. The 2.5 MW ECCD could still suppress the island width to $0.03a$ when w_{cd} is increased by 0.5 times, meaning that the ECCD reduces the magnetic island width by 3/4 in such a case. Figure 6 also indicates that (2,1) mode is more difficult to be suppressed than (3,2) mode, and has a greater deleterious impact on plasma performance improvement, which is consistent with the results from La Haye.[36] It is also should be noted that our simulation considers the NTM with neoclassical effect, because if the bootstrap current is not considered, the magnetic island saturation will be lower than the magnetic island saturation level presently here. Especially for the (3,2) mode, if the neoclassical effect of the bootstrap current is not incorporated, the tearing mode will not be excited.

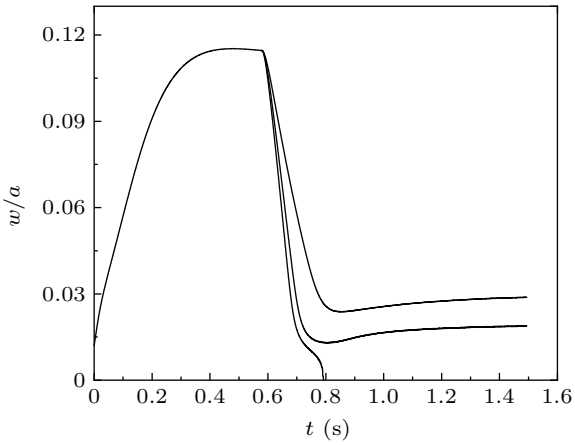


Fig. 6. The same as in Fig. 4, but for (3,2) NTM control.

3.3. Time needed to suppress the neoclassical tearing mode

Now we come to study the time needed to suppress both the (3,2) and (2,1) mode systematically. Figure 7 shows the time necessary to reduce the island to 1/3 of its initial size (solid line) and for complete stabilization (dashed line) versus ECW power, for both the (3,2) mode (a) and the (2,1) mode (b). It demonstrates that the time required for suppression of (3,2) mode is shorter than that for (2,1) mode. The time required to completely suppress (2,1) mode is about 0.2 s, while it is 0.128 s that required to suppress (3,2) mode when the power is 3.0 MW. Overall, the time for suppress of (3,2) mode shorter. This is reasonable since the bootstrap current is significantly larger at the $q = 2/1$ than that at the $q = 3/2$ surface, and thus the current to be replaced is larger and the power needed is larger as well. In other words, the time needed for (3,2) mode suppress should be shorter when input wave power are the same. On the other hand, when one reduces the magnetic island to 1/3 of the saturation value, similarly, the suppression time could also be shortened.

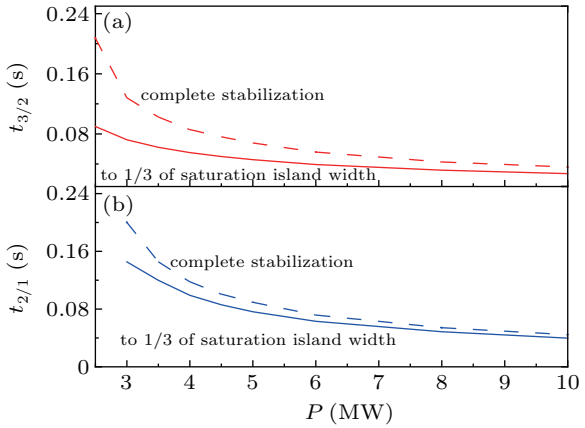


Fig. 7. Time necessary to reduce the island to 1/3 of saturation island width value (solid line) and for complete stabilization (dashed line) versus ECW power, for both the (3,2) mode (a) and the (2,1) mode (b).

Time needed for complete stabilization versus initial island width (normalized to the saturation width) is shown in Fig. 8 for both the (2,1) and the (3,2) modes. It can be seen that the earlier the ECCD is placed, the shorter the time needed to fully suppress NTM. The relationship between the required time and $w_{\rm ini}$ is linear for (3,2) mode, while there is also a weak linear relationship for (2,1) mode. What should be noted is that the input power in Fig. 8 is 5 MW. One can still see that the time for suppression of (3,2) mode is shorter than the that for (2,1) mode. The time required for suppression of the two is very close when the initial magnetic island is small. This result seems similar to the simulation result in ITER.[37]

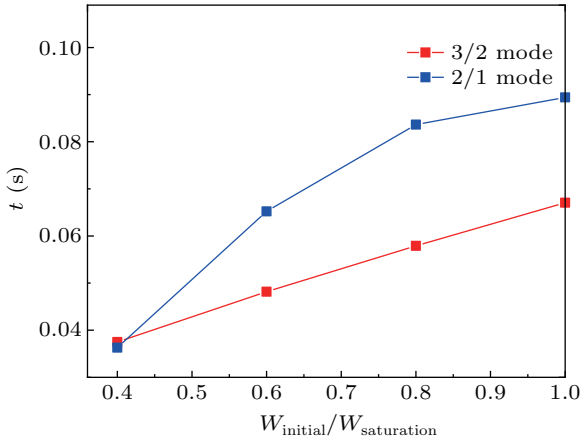


Fig. 8. Time needed for complete stabilization versus ECW initial island width (the island width when ECW power is added, normalized to the saturation width), for both the (2,1) and the (3,2) modes.

4. Conclusion

Investigation of neoclassical tearing mode and its suppression by electron cyclotron current drive (ECCD) have been performed for HL-2M tokamak. The electron cyclotron wave driven current capability is evaluated. It is found that the deposition location can be effectively controlled by changing poloidal injection angle. The validation of electron cyclotron wave heating and current drive has been demonstrated for the upper launcher port. The required poloidal injection angle range is about 30° (from 98° to 128°) in order to cover the radial range of $\rho = 0.5$–0.9. The absorption of the wave power reaches 100%, while current drive efficiencies reach the order of 0.014×10^{20} A/W/m^2 with the upper launcher emission.

For the NTM suppression, we show that 3.0 MW and 2.5 MW modulated ECCD can completely stabilize (2,1) and (3,2) NTMs, respectively. The non-modulated ECCD, radial misalignment as well as current profile broadening have deleterious effect on the NTM stabilization. The time required for suppression of (3,2) mode is shorter than that required for the suppression of (2,1) mode. We find that the earlier the ECCD is placed, the shorter the time needed to fully suppress NTM. And the relationship between the required time and $w_{\rm ini}$ is basically linear.

In general, the total electron cyclotron wave current of 5 MW is sufficient to have a full stabilization of both (2,1) and (3,2) modes. In addition, the plasma temperature we set is lower than the expected when calculating the ECCD. From the current expected parameters, the plasma center temperature of HL-2M will be higher than 6 keV. Increasing the temperature will significant increase the current drive efficiency. Therefore, our simulation here gives a conservative EC wave power input for full suppression of (2,1) and (3,2) modes. Up to 30% higher CD efficiencies are predicted if the plasma has a core temperature of 10 keV, at the cost of higher ohmic heating and other auxiliary heating.

Acknowledgments

The authors would like to thank X. Wang at HIT, Min Xu at SWIP, Q. Yu, X. Wang, and L. Xue for fruitful discussions. J. C. Li also thanks the High-performance Computing Platform of Peking University.

References

[1] Sauter O, LaHaye R J, Chang Z, *et al.* 1997 *Phys. Plasmas* **4** 1654
[2] La Haye R J, Lao L L, Strait E J and Taylor T S 1997 *Nucl. Fusion* **37** 397
[3] Giruzzi G, Zabiego M, Gianakon T A, Garbet X, Cardinali A and Bernabei S 1999 *Nucl. Fusion* **39** 107
[4] Li J C, Xiao C J, Lin Z H and Wang K J 2017 *Phys. Plasmas* **24** 082508
[5] Zohma H, Gantenbeinb G, Gudea A, Gnter S, Leuterera F, Marascheka M, P. Meskatb J, Suttropa W, Yu Q and ASDEX Upgrade Team 2001 *Nucl. Fusion* **41** 197
[6] Poli E, Tardini G, Zohm H, Fable E, Farina D, Figini L, Marushchenko N B and Porte L 2013 *Nucl. Fusion* **53** 013011
[7] Pinsker R I 2001 *Phys. Plasmas* **8** 1219
[8] Wei W, Ding B J, Peysson Y, Decker J, Li M H, Zhang X J, Wang X J and Zhang L 2016 *Chin. Phys. B* **25** 015201
[9] Fitzpatrick R 1993 *Nucl. Fusion* **33** 1049
[10] Yu Q, Gunter S and Lackner K 2018 *Nucl. Fusion* **58** 054003
[11] Prater R 2004 *Phys. Plasma* **11** 2349
[12] Gantenbein G, Zohm H, Giruzzi G, Gunter S, Leuterer F, Maraschek M, Meskat J, Yu Q, ASDEX Upgrade Team and ECRH-Group 2000 *Phys. Rev. Lett.* **85** 1242
[13] Petty C C, La Haye R J, Luce T C, Humphreys D A, Hyatt A W, Lohr J, Prater R, Strait E J and Wade M R 2004 *Nucl. Fusion* **44** 243

[14] Isayama A, Kamada Y, Ozeki T, Ide S, Fujita T, Oikawa T, Suzuki T, Neyatani Y, Isei N, Hamamatsu K, Ikeda Y, Takahashi K, Kajiwara K and JT-60 Team 2001 *Nucl. Fusion* **41** 761
[15] Yan L, Ji X, Song S, *et al.* 2017 *Rev. Sci. Instrum.* **88** 113504
[16] Shi T H, Wan B N, Shen B, *et al.* 2013 *Plasma Phys. Control. Fusion* **55** 055007
[17] Welander A S, Kolemen E, La Haye R J, Eidietis N W, Humphreys D A, Lohr J, Noraky S, Penaflor B G, Prater R and Turco F 2013 *Plasma Phys. Control. Fusion* **55** 124033
[18] Bardoczi L, Choi M J, Navarro A B, Shiraki D, La Haye R J, Park S H, Knolker M, Evans T E, McKee G R, Woo M, Park B H and Jenko F 2019 *Nucl. Fusion* **59** 126047
[19] Sauter O, Buttery R J, Felton R, Hender T C, Howell D F and contributors to the EFDA-JET Workprogramme 2002 *Plasma Phys. Control. Fusion* **44** 1999
[20] La Haye R J, Prater R, Buttery R J, Hayashi N, Isayama A, Maraschek M E, Urso L and Zohm H 2006 *Nucl. Fusion* **46** 451
[21] Westehof E, de Blank H J and J Pratt 2016 *Nucl. Fusion* **56** 036016
[22] Maget P, Fevrier O, Garbet X, Lutjens H, Luciani J F and Marx A 2016 *Nucl. Fusion* **56** 086004
[23] Poli E, Bottino A, Hornsby W A, Peeters A G, Ribeiro T, Scott B D and Siccinio M 2010 *Plasma Phys. Control. Fusion* **52** 124021
[24] Hornsby W A, Migliano P, Buchholz R, Grosshauser S, Weikl A, Zarzoso D, Casson F J, Poli E and Peeters A G 2016 *Plasma Phys. Control. Fusion* **58** 014028
[25] Li J C, Xiao C J, Lin Z H, Liu D J, Ji X Q and Wang X G 2020 *Phys. Plasmas* **27** 042507
[26] Li J G and Wan Y X 2019 *Journal of Fusion Energy* **38** 113
[27] Li J C, Ding X T, Dong J Q and Liu S F 2020 *Plasma Phys. Control. Fusion* **62** 095013
[28] Xia F, Pan L, Zhao L, Pan W, Song X, Li X Y, Wang C, Lan J T, Chen L Y and Nakamura K 2012 *Plasma and Fusion Research* **7** 2405048
[29] Lin-Liu Y R, Chan V S and Prater R 2003 *Phys. Plasmas* **10** 4064
[30] Merkulov A, Westepf E, Schuller F C, de Baar M R, Kramer-Flecken A, Liang Y and TEXTOR Team 2004 *Proc. Joint Varenna-Lausanne Int. Workshop on Theory of Fusion Plasmas*, Varenna, Italy p. 279
[31] Ramponi G, Farina D, Henderson A M, Poli E, Saibene G and Zohm H 2007 *Fusion Sci. Technol.* **52** 193
[32] Li J C, Gong X Y, Dong J Q, Zheng P W, Song S D, Gao Q D and Du D 2015 *Phys. Plasmas* **22** 062512
[33] Yu Q, Zhang X D and Gunter S 2004 *Phys. Plasmas* **11** 1960
[34] Lao L L, John H St, Stambaugh R D, Kellman A G and Pfeiffer W 1985 *Nucl. Fusion* **25** 1611
[35] Li J C, Gong X Y, Dong J Q, Wang J and Yin L 2016 *Chin. Phys. B* **25** 045201
[36] La Haye R J, Isayama A and Maraschek M 2009 *Nucl. Fusion* **49** 045005
[37] Giruzzi G and Zabiego M 2001 *Fusion Engineering and Design* **53** 43